01 Jan 2017

Expedite Design of Variable-Topology Broadband Hybrid Couplers for Size Reduction using Surrogate-Based Optimization and Co-Simulation Coarse Models

Piotr Kurgan

Slawomir Koziel

Leifur Leifsson

Xiaosong Du
Missouri University of Science and Technology, xdnwp@mst.edu

Recommended Citation

P. Kurgan et al., "Expedite Design of Variable-Topology Broadband Hybrid Couplers for Size Reduction using Surrogate-Based Optimization and Co-Simulation Coarse Models," *Procedia Computer Science*, vol. 108, pp. 1483 - 1492, Elsevier, Jan 2017.
The definitive version is available at https://doi.org/10.1016/j.procs.2017.05.071

Available online at www.sciencedirect.com

ScienceDirect

Procedia Computer Science 108C (2017) 1483–1492

Procedia Computer Science

International Conference on Computational Science, ICCS 2017, 12-14 June 2017, Zurich, Switzerland

Expedite Design of Variable-Topology Broadband Hybrid Couplers for Size Reduction Using Surrogate-Based Optimization and Co-Simulation Coarse Models

Piotr Kurgan[1#] Slawomir Koziel[1*], and Leifur Leifsson[2†], and Xiaosong Du[2‡]

[1]*Reykjavik University, Iceland*

[2]*Iowa State University, USA*

kurgan@ru.is, koziel@ru.is, leifur@iastate.edu, xiaosong@iastate.edu

Abstract

In this paper, we discuss a computationally efficient approach to expedite design optimization of broadband hybrid couplers occupying a minimized substrate area. Structure size reduction is achieved here by decomposing an original coupler circuit into low- and high-impedance components and replacing them with electrically equivalent slow-wave lines with reduced physical dimensions. The main challenge is reliable design of computationally demanding low-impedance slow-wave structures that feature a quasi-periodic circuit topology for wideband operation. Our goal is to determine an adequate number of recurrent unit elements as well as to adjust their designable parameters so that the coupler footprint area is minimal. The proposed method involves using surrogate-based optimization with a reconfigurable co-simulation coarse model as the key component enabling design process acceleration. The latter model is composed in Keysight ADS circuit simulator from multiple EM-evaluated data blocks of the slow-wave unit element and theory-based feeding line models. The embedded optimization algorithm is a trust-region-based gradient search with coarse model Jacobian estimation. We exploit a penalty function approach to ensure that the electrical conditions for the slow-wave lines are accordingly satisfied, apart from explicitly minimizing the area of the coupler. The effectiveness of the proposed technique is demonstrated through a design example of two-section 3-dB branch-line coupler. For the given example, we obtain nine circuit design solutions that correspond to the compact couplers whose multi-element slow-wave lines are composed of unit cells ranging from two to ten.

Keywords: branch-line couplers, compact couplers, co-simulation modeling, electromagnetic simulations, surrogate-based optimization.

Engineering Optimization & Modeling Center, School of Science and Engineering
* Engineering Optimization & Modeling Center, School of Science and Engineering
† Department of Aerospace Engineering, 2271 Howe Hall, Ames, IA, 50011, USA
‡ Department of Aerospace Engineering

10.1016/j.procs.2017.05.071

1 Introduction

Hybrid directional couplers are prominent microwave components, finding diverse applications in balanced-type circuits such as power amplifiers (Malo-Gomez et al., 2009; Wincza and Gruszczynski, 2011), mixers (Lin et al., 2008; Shahroury and Wu, 2008) or antenna feeding systems (Wincza and Gruszczynski, 2016; Lin et al., 2013) to name just a few. The most representative examples of hybrid (that is offering an equal power division between the output ports) couplers include branch-line couplers (Mongia, Bahl and Bhartia, 1999) and rat-race couplers (Xu, Wang and Lu, 2011). For circuit implementation realized in planar technologies, the branch-line couplers are typically chosen over the rat-race couplers as the output arms of the latter devices are separated by an isolated port (Muraguchi, Yukitake and Naito, 1983). The drawbacks include an increased design complexity as well as an elevated estate area consumption, both resulting from the necessity of using crossovers (normally realized as hybrid couplers in a back-to-back configuration) to comply with requirements of planar technologies (Wong and Cheng, 2011). The classic textbook design formulas for the branch-line couplers provide a perfect matching and isolation of the circuit as well as an even power split with a 90-degree phase difference between the outputs (Pozar, 1998). However, this ideal circuit operation is only attainable at a single frequency (typically the center of the functional bandwidth) and deteriorates with the departure from the operating point. In a basic one-section circuit configuration, branch-line couplers offer an acceptable performance over an inherently narrow band of about 10% (Mongia, Bahl and Bhartia, 1999). The latter is due to the modular architecture of the discussed type of directional couplers, which is primarily based on quarter-wavelength transmission lines. Another downside of such a circuit topology is a large footprint area, which becomes a particular issue for space-limited applications of the lower microwave spectrum. The aforementioned problems have encouraged continued efforts to obtain compact branch-line coupler design solutions with a wideband operation (Chun and Hong, 2006; Yao, 2010; Lee and Lee, 2012; Ariolla, Lee and Kim, 2011). Size reduction of the structure under development is typically accomplished by replacing conventional lines of the original device with slow-wave lines with intricate geometries (Lee and Lee, 2012). Unfortunately, this raises issues related to the selection (or development) of proper simulation models for accurate (yet feasible) circuit performance evaluation. On one hand, electromagnetic (EM) computational models are reliable, but expensive. On the other hand, equivalent circuits are merely capable of delivering a rough approximation of a design solution. The given design problem becomes even more challenging when considered from the wideband application standpoint. In general, broadband transmission characteristics are available using multi-element slow-wave structures so that the corresponding design task in not only associated with adjustment of (continuous) geometry parameters, but—most importantly—with determination of the (discreet) number of duplicated slow-wave unit elements. The very problem has been previously approached by using surrogate-based optimization with kriging interpolation models (Kurgan, Koziel and Bandler, 2016). The development of multi-dimensional data-driven models—fairly accurate over a wide-ranged parameter space—is a challenging task itself and typically requires an additional fine-tuning, which adds notably to the total computational design cost.

This work presents the effectiveness of applying the co-simulation models—combining the accuracy of EM analysis and cost-efficiency of circuit simulation—in the process of expedited and reliable design optimization of multi-element slow-wave structures to be used as the key building blocks of compact wideband hybrid couplers. Our methodology, involving a trust-region gradient search with Jacobian estimation embedded in a surrogate-based optimization scheme, is used here to obtain nine design solutions at a moderate CPU cost. The final design with the smallest circuit area requires no further fine-tuning.

2 The Design Problem: Variable-Topology Broadband Coupler

This work aims at addressing the design problem of broadband equal-split branch-line couplers with compact footprints. The miniaturization concept applied here is based on the decomposition of a reference structure (typically, an analytical or numerical design solution of an ideal circuit model) and replacement of its building blocks with electrically equivalent, but shortened transmission lines featuring a slow-wave effect (Kurgan, Filipcewicz and Kitlinski, 2012).

Here, the original circuit model is an ideal two-section branch-line coupler shown in Fig. 1. It consists of low- (Z_L) and high-impedance (Z_H) quarter-wavelength transmission lines. As indicated by the results reported in (Kurgan, Koziel and Bandler, 2016), the device under discussion offers an infinite number of solutions that satisfy the following requirements for an ideal hybrid branch-line coupler: (i) an even power division between the direct and coupled ports at the operating frequency f_0, (ii) matching and isolation better than –20 dB at f_0, and (iii) a –90° phase difference between the coupled and direct ports at f_0. For the purpose of our further considerations, we hand-pick a specific design solution for that structure using a design chart of (Kurgan, Koziel and Bandler, 2016), namely, $Z_L = 34\ \Omega$ and $Z_H = 116.19\ \Omega$.

The principal stage of the miniaturization procedure adopted here is finding suitable slow-wave substitutes for the conventional transmission lines that constitute the original coupler. This way the performance of the reference circuit can be maintained by satisfying design requirements imposed on its building blocks. As thoroughly discussed in the literature (Kurgan, Filipcewicz and Kitlinski, 2012), designing of low-impedance slow-wave structures for wideband operation is particularly difficult due to a large number of parameters describing their geometrically intricate layouts, the necessity of using a multi-element topology instead of an inherently narrowband single-element one to provide an enhanced bandwidth as well as a high computational cost of the corresponding EM-simulated models. To this end, we consider a cascade of a variable number of slow-wave unit elements with additional feeding line sections placed at both ends (see Fig. 2). The proposed low-impedance slow-wave line is sufficiently described by a vector of eight continuous geometry parameters $\boldsymbol{x}_c = [l_1\ l_2\ l_3\ w_1\ w_2\ w_3\ w_4\ g]^T$ and a discreet multiplication factor n. One should observe that the arrangement of the low-impedance lines in the original circuit ensures that the dimensions of the target compact coupler are dependent exclusively on $\boldsymbol{x}_c$, provided that the high-impedance lines are simply folded to the interior of the structure.

The goal of the design procedure is to find values of $\boldsymbol{x}_c$ and n that minimize the coupler area and provide proper electrical parameters of its building blocks (in particular, an appropriate impedance and electrical length).

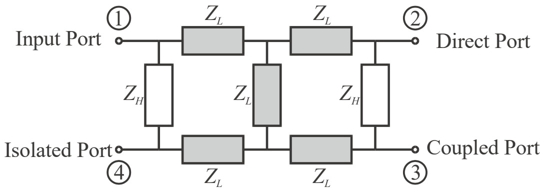

Figure 1: Two-section branch-line coupler composed of ideal, quarter-wavelength transmission lines of low (Z_L) and high impedance (Z_H).

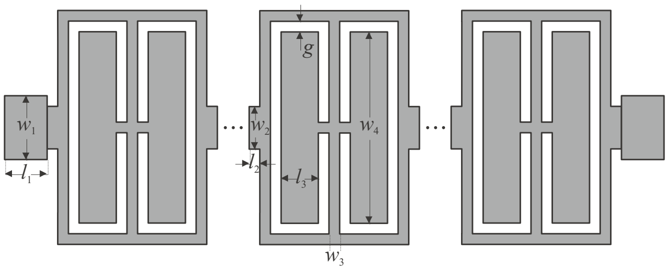

Figure 2: Layout of a variable-topology cascade of n slow-wave unit elements with feeding lines placed at each end.

3 Design Optimization Procedure

In this section we outline a procedure developed to handle the design optimization task discussed in Section 2. The fundamental issue is low-cost optimization of cascaded slow-wave structures as fundamental building blocks of the compact wideband couplers (cf. Section 2). It should be emphasized that the procedure is focused both on explicit size reduction of the coupler footprint area and, at the same time, on satisfying electrical performance parameters. At the level of the cascaded slow-wave structure these are the characteristic impedance and its phase shift. The entire optimization process is repeated for all considered multiplication factors (from 2 to 10) in order to identify the overall best coupler topology.

3.1 Low-Fidelity Models for Cascade Optimization

One of our primary goals is to conduct the design optimization process in a computationally feasible manner. To accomplish this, we utilize a surrogate-based optimization paradigm (Koziel and Leifsson, 2016). The main challenge is the design of a cascade of slow-wave compact cells that substitutes for low-impedance lines of the original wideband coupler. Here, we develop a co-simulation coarse model $\boldsymbol{c}$ of the discussed cascade as shown in Fig. 3. It is implemented in Keysight ADS (ADS, 2011) and contains five duplicated cells, with feeding lines placed at each end. The cells are represented as EM-simulated data components included in the co-simulation model of the cascade.

The benefit of using the co-simulation model is that its computational cost is the same as the cost of evaluating a single cell, which is considerably lower than the cost of EM analysis of the entire cascade. Clearly, due to the fact that cross-coupling effects between the cells are neglected in the co-simulation model, a correction is needed to improve its accuracy and use it in the design process.

3.2 Formulation of the Objective Function

There are three major objectives of the design procedure. These are as follows (here, $\boldsymbol{x}_c$ denotes a vector of geometry parameters of the slow-wave cascade, cf. Section 2):

1. Reduce the overall footprint area of the coupler $A(\boldsymbol{x}_c)$;
2. Obtain a required phase shift of –90° between the input and the output of the cascade at the operating frequency f_0;
3. Maintain the maximum return loss level of –30 dB for the cascade, over the bandwidth of interest.

The goal is to design area-efficient counterparts for the components of the original coupler circuit of Fig. 1, fulfilling the above-listed requirements. Here, the focus is on design of the cascaded slow-wave structure, due to its computational demands, however, the design optimization of the folded high-impedance branch is accomplished in a similar manner (excluding the first objective). One should note that the high-impedance branch is geometrically simple so that the corresponding EM model is sufficiently cheap to be used directly. All of these goals can be achieved by minimizing the following objective function:

$$U(\boldsymbol{x}) = A(\boldsymbol{x}) + \beta_1[(P(\boldsymbol{x}_c) + 90)/90]^2 + \beta_2[\max(S(\boldsymbol{x}_c) + 30, 0)/30]^2 \tag{1}$$

where $P(\boldsymbol{x}_c)$ and $S(\boldsymbol{x}_c)$ are the cascade phase shift (at f_0) and its return loss (over a frequency band of interest), respectively, evaluated from EM-simulated cascade model $\boldsymbol{f}$. The first penalty term in (1) enforces a required value of –90° for the transmission phase; the second term contributes to the main objective in case the return loss requirement is violated; β_k, $k = 1, 2$, are penalty coefficients.

3.3 Optimization Algorithm

The coupler design problem is formulated as a nonlinear minimization task of the form

$$\boldsymbol{x}^* = \arg\min_{\boldsymbol{x}} U(\boldsymbol{x}) \tag{2}$$

Here, we solve it iteratively using a trust-region (TR)-embedded (Conn *et al.*, 2000) gradient search algorithm that generates a sequence of approximations $\boldsymbol{x}^{(i)}$, $i = 0, 1, \ldots$, to $\boldsymbol{x}^*$

$$\boldsymbol{x}^{(i+1)} = \arg\min_{\boldsymbol{x};\, \|\boldsymbol{x}-\boldsymbol{x}^{(i)}\| \le \delta^{(i)}} L_c^{(i)}(\boldsymbol{x}) \tag{3}$$

where $\delta^{(i)}$ is the trust region radius at iteration i updated using standard TR rules (Conn *et al.*, 2000). The model $L_c^{(i)}$ is defined as

$$L_c^{(i)}(\boldsymbol{x}) = A(\boldsymbol{x}) + \beta_1[(L_P^{(i)}(\boldsymbol{x}_c) + 90)/90]^2 + \beta_2[\max(L_S^{(i)}(\boldsymbol{x}_c) + 30, 0)/30]^2 \tag{4}$$

with

$$L_P^{(i)}(\boldsymbol{x}) = P(\boldsymbol{x}_c^{(i)}) + J_{c.P}(\boldsymbol{x}_c^{(i)}) \cdot (\boldsymbol{x} - \boldsymbol{x}_c^{(i)}) \tag{5}$$

$$L_S^{(i)}(\boldsymbol{x}) = S(\boldsymbol{x}_c^{(i)}) + J_{c.S}(\boldsymbol{x}_c^{(i)}) \cdot (\boldsymbol{x} - \boldsymbol{x}_c^{(i)}) \tag{6}$$

being linear expansions of P and S at $\boldsymbol{x}_c^{(i)}$. Here, the Jacobians $J_{c.P}$ and $J_{c.S}$ are estimated through finite differences of the co-simulation coarse model $\boldsymbol{c}$. In other words, we have

$$J_{c.P}(\boldsymbol{x}_c^{(i)}) = \begin{bmatrix} \dfrac{P(\boldsymbol{x}_c^{(i)} + \boldsymbol{h}_1) - P(\boldsymbol{x}_c^{(i)})}{h_1} \\ \vdots \\ \dfrac{P(\boldsymbol{x}_c^{(i)} + \boldsymbol{h}_n) - P(\boldsymbol{x}_c^{(i)})}{h_n} \end{bmatrix}^T \tag{7}$$

and

$$J_{c.S}(\boldsymbol{x}_c^{(i)}) = \begin{bmatrix} \dfrac{S(\boldsymbol{x}_c^{(i)}+\boldsymbol{h}_1)-S(\boldsymbol{x}_c^{(i)})}{h_1} \\ \vdots \\ \dfrac{S(\boldsymbol{x}_c^{(i)}+\boldsymbol{h}_n)-S(\boldsymbol{x}_c^{(i)})}{h_n} \end{bmatrix}^T \tag{8}$$

where h_k, $k = 1, \ldots, n$, are finite difference step sizes (due to numerical noise in EM simulation results, we choose relatively large values of h_k such as 10^{-2}), whereas $\boldsymbol{h}_k = [0 \ldots 0\ h_k\ 0 \ldots 0]^T$ with h_k on the kth position.

Note that although the low- and high-fidelity cascade models $\boldsymbol{c}$ and $\boldsymbol{f}$ are misaligned, they are normally well correlated so that the Jacobian estimation using low-fidelity model can be considered as reliable. It should also be noted that each iteration of (3) requires just one EM simulation of the cascade.

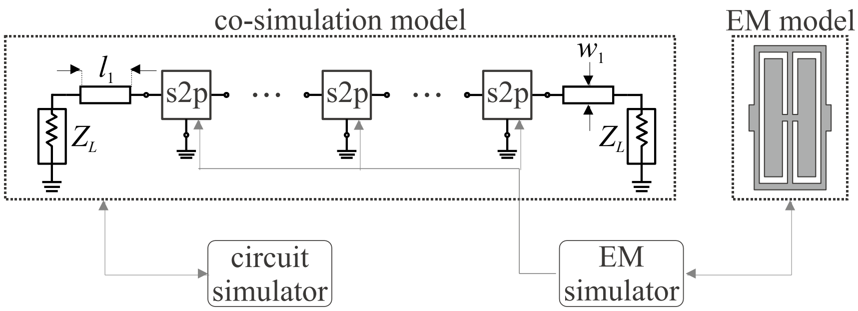

Figure 3: Co-simulation ADS model of variable-topology n-element cascade of slow-wave unit elements with feeding lines placed at each end. Note that the structure is terminated with Z_L impedances so that keeping the maximum return loss level at –30 dB in the given band of interest ensures that the cascade characteristic impedance approaches Z_L.

4 Results and Discussion

The design problem outlined in Section II is addressed here by following the proposed methodology detailed in Section III. The development of a compact coupler with a wideband operation and minimized layout area is divided into two parts. The primary task is to adjust the designable parameters of the variable-topology low-impedance slow-wave structure of Fig. 2 so that the coupler layout area is minimized with simultaneous ensuring of proper electrical parameters, that is, the characteristic impedance Z_L and –90° phase shift. These objectives are accomplished by executing (3)–(6) for each considered n (here, n ranges from 2 to 10). The final compact coupler is selected as the one with the smallest layout area among all obtained design solutions. The secondary task is to adjust geometry parameters of the folded high-impedance branch by completing objectives (2)–(3) from Section 3.2. This can be done directly using conventional optimization algorithms as the corresponding EM problem is not computationally demanding.

For solving the design example described in this section, we choose the Taconic RF-35 dielectric substrate with effective permittivity of 3.5 and substrate height of 0.762 mm. The operating frequency for the original coupler circuit and its small-size versions is set to f_0 = 1 GHz. In addition, we use microstrip technology for all circuit implementations. For comparison purposes, a microstrip realization of the original two-section branch-line coupler at f_0 = 1 GHz occupies an excessive estate area of 91.7 mm × 51.0 mm (4677 mm^2).

All simulation models utilized within the proposed design method are implemented in CST EM simulation environment (CST, 2013) with fine accuracy settings. The present design example as described above requires the development of several EM models, in particular: a slow-wave unit element model, slow-wave cascade models (for each considered n; nine models in total), and a compact coupler model (for n that minimizes coupler layout area). An average simulation time of the above listed models (calculated as the mean of all conducted simulations) is, approximately, 85, 770, and 1750 (all in seconds), respectively. The lower and upper bounds $\boldsymbol{l}/\boldsymbol{u}$ for the design space of x_c, together with the starting point $\boldsymbol{x}_c^{(0)}$ are collected in Table I.

We repeat the proposed design optimization procedure for all considered values of n. The obtained numerical results are shown in Table II. Note that the scale of miniaturization included in the comparison is calculated based on to the 4677-mm^2 layout size of the original coupler microstrip realization. The numerical cost of acquiring the results of Table II corresponds to 95 simulations of the high-fidelity EM model of the compact coupler with three-element low-impedance cascades (note that the smallest coupler layout area is reached with n = 3). A detailed breakdown of the design cost of low-impedance slow-wave structure optimization is presented in Table III, where N_c and N_f stand for the number of simulations pertaining to c and f models, respectively, while $\boldsymbol{R}_f$ represents the compact coupler model for n = 3.

Table I: Lower/upper bounds $\boldsymbol{l}/\boldsymbol{u}$ and the starting point $\boldsymbol{x}_c^{(0)}$ for cascade optimization

	Design variables							
	l_1	l_2	l_3	w_1	w_2	w_3	w_4	g
$\boldsymbol{l}$	0.1	0.5	0.1	0.1	0.5	0.1	0.5	0.1
$\boldsymbol{u}$	5.0	3.5	0.5	1.0	2.0	0.5	10.0	1.0
$\boldsymbol{x}_c^{(0)}$	2.55	2.0	0.3	0.55	1.25	0.3	5.25	0.55

Table II: Numerical results of low-impedance slow-wave structure design optimization

n	A [mm^2]	Miniaturization [%]	Design variables							
			l_1	l_2	l_3	w_1	w_2	w_3	w_4	g
2	1376	70.0	5.8	0.1	0.95	1.0	0.2	0.43	11.15	0.19
3	1299	71.7	2.85	0.1	0.78	6.95	0.48	0.32	11.61	0.1
4	1323	71.2	2.47	0.1	0.32	7.62	1.55	0.42	11.31	0.1
5	1366	70.2	2.83	0.1	0.3	4.5	1.47	0.44	8.87	0.1
6	1375	70.0	1.04	0.1	0.23	8.75	3.28	0.38	9.68	0.1
7	2093	54.4	2.57	0.1	0.47	2.46	1.76	0.53	4.77	0.12
8	1776	61.3	2.57	0.1	0.1	1.0	0.74	0.61	4.52	0.1
9	1422	69.0	3.55	0.1	0.1	1.0	5.0	0.29	7.13	0.1
10	1305	71.6	4.58	0.1	0.1	1.0	9.24	0.1	9.55	0.1

Table III: Numerical cost of low-impedance slow-wave structure design optimization

n	N_c	N_f	Total [min]	Total in $\boldsymbol{R_f}$
2	48	8	171	5.85
3	51	11	213	7.32
4	59	11	225	7.71
5	87	14	303	10.39
6	104	16	353	12.09
7	39	7	145	4.97
8	129	25	504	17.27
9	160	24	535	18.33
10	95	15	327	11.21
Collective cost				95.14

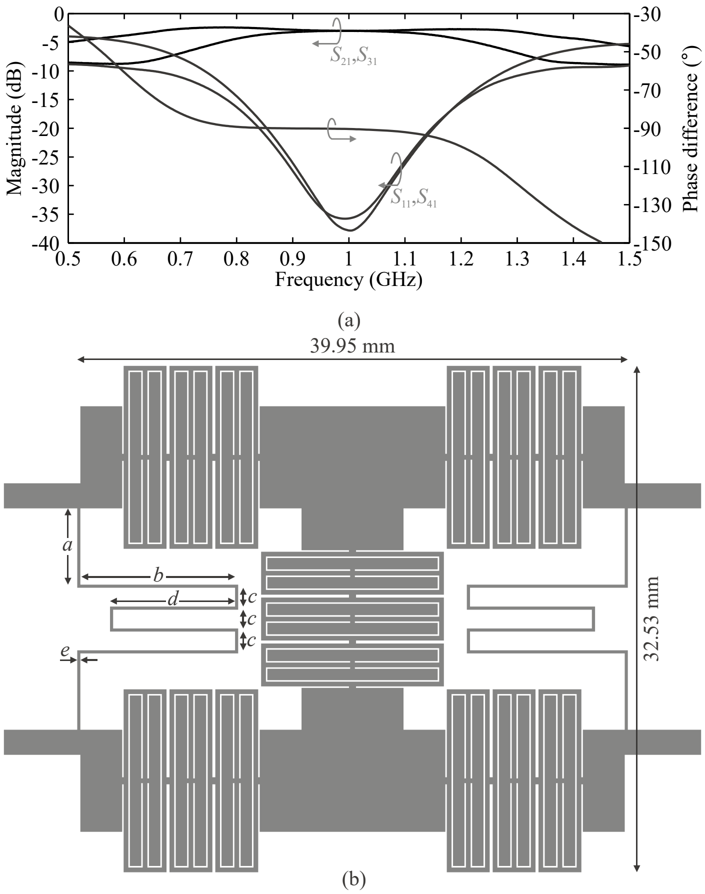

Figure 4: (a) EM-validated frequency performance of the final compact coupler (magnitude of S-parameters of the left axis and phase difference between the coupled and direct ports on the right axis); (b) Layout of the smallest compact coupler: $a = 4.15$, $b = 8.41$, $c = 1.02$, $d = 6.64$, $e = 0.21$(all dimensions in millimeters).

The secondary stage of the design procedure involves obtaining a folded high-impedance branch that matches the low-impedance design solution with the smallest layout area ($n = 3$). Taking the case of $n = 3$ independently, the entire design cost of obtaining the compact coupler corresponds to 11.18 $\boldsymbol{R_f}$ (which includes design optimization of the high-impedance branch and the final compact coupler evaluation). This result has been obtained efficiently when compared to a direct EM optimization of the compact coupler with 12 designable parameters (8 for the low-impedance line and 4 for the high-impedance branch), whose estimated design cost is 150 $\boldsymbol{R}_f$.

The frequency characteristics as well as the layout of the final compact coupler are depicted in Fig. 4. Note that the simulated coupler performance shown in Fig. 4(a) confirms that the proposed design optimization methodology is very accurate, as no additional CPU-expensive design closure is required. The final coupler shown in Fig. 4(b) occupies a small circuit area of 28.3% of the original coupler microstrip realization. It also illustrates a high performance, that is, an even power split at the operating frequency ($|S_{21}|$, $|S_{31}|$ = –3.02 dB) and a –90.0° phase difference between the coupled and direct output ports at f_0. In addition, the couple offers a wide fractional bandwidth of 31.1% (calculated for the return loss and isolation ≤–20 dB).

5 Conclusion

This work presents a reliable design methodology for broadband hybrid couplers whose topologies are adjusted in the process of coupler layout minimization. The application of accurate, yet computationally cheap co-simulation models and surrogate-based optimization enables keeps the numerical expenditure at a low level. The final coupler offers a small size and a high performance, without additional fine-tuning.

Acknowledgement

The authors would like to thank Computer Simulation Technology AG, Darmstadt, Germany, for making CST Microwave Studio available. This work has been partially supported by the Icelandic Centre for Research (RANNIS) Grant 163299051.

References

Advanced Design System (ADS), ver. 2011.10, 2011, Agilent Technologies, 1400 Fountaingrove Parkway. Santa Rosa, CA.

Arriola, W.A., Lee, J.Y., Kim, I.S. (2011) “Wideband 3 dB branch line coupler based on λ/4 open circuited coupled lines,” *IEEE Microw. Wireless Comp. Lett.*, vol. 21, no. 9, pp. 486–488.

Chun, Y.-H., Hong, J.-S. (2005) “Design of a compact broadband branch-line hybrid,” *IEEE MTT-S Int. Microw. Symp.* pp. 997–1000.

Chun, Y.-H., Hong, J.-S. (2006) “Compact wide-band branch-line hybrids,” *IEEE Trans. Microw. Theory Tech.*, vol. 54, no. 2, pp. 704–709.

Conn, A.R., Gould, N.I.M., Toint, P.L. (2000), *Trust Region Methods*, 2000 MPS-SIAM Series on Optimization.

CST Microwave Studio, ver. 2013, CST AG, Bad Nauheimer Str. 19, D-64289 Darmstadt, Germany, 2013.

Echeverria, D., Hemker, P.W. (2005) *Space mapping and defect correction*. CMAM Int. Mathematical Journal Computational Methods in Applied Mathematics, 5, 107–136.

Koziel, S., Bekasiewicz, A. (2015) “Fast EM-driven size reduction of antenna structures by means of adjoint sensitivities and trust regions,” *IEEE Ant. Wireless Prop. Lett.*, vol. 14, pp. 1681–1684.

Koziel, S., Leifsson, L. (2016), *Simulation-driven Design by Knowledge-based Response Correction Techniques*, Springer, New York.

Kurgan, P., Filipcewicz, J., Kilinski, M. (2012) "Development of a compac microstrip resonan cell aimed a efficien microwave component size reducion," *IET Microw. Ant. Propag.*, vol. 6, no. 12, pp. 1291–1298.

Kurgan, P., Koziel, S., Bandler, J.W. (2016) "Surrogate-based miniaturization-oriented design of two-section branch-line couplers," *2016 IEEE MTT-S Int. Microwave Symp. (IMS)*, pp. 1–3.

Lee, S., Lee, Y. (2012) "Wideband branch-line couplers with single-section quarter-wave transformers for arbitrary coupling levels," *IEEE Microw. Wireless Comp. Lett.*, vol. 22, no. 1, pp. 19–21.

Lin, C.-M., Lin, H.-K., Lin, C.-F., Lai, Y.-A., Lin, C.-H., Wang, Y.-H. (2008) "A 16–44 GHz compact doubly balanced monolithic ring mixer," *IEEE Microw. Wireless Comp. Lett.*, vol. 18, no. 9, pp. 620–622.

Lin T.-H., Hsu, S.-K., Wu, T.-L. (2013) "Bandwidth enhancement of 4×4 Butler matrix using broadband forward-wave directional coupler and phase difference compensation," *IEEE Trans. Microw. Theory Tech.*, vol. 61, no. 12, pp. 4099–4109.

Malo-Gomez, I., Gallego-Puyol, J.D., Diez-Gonzalez, C., Lopez-Fernandez, I., Briso-Rodriguez, C. (2009) "Cryogenic hybrid coupler for ultra-low-noise radio astronomy balanced amplifiers," *IEEE Trans. Microw. Theory Tech.*, vol. 57, no. 12, pp. 3239–3245.

Mongia, R., Bahl, I., Bhartia, P. (1999) *RF and microwave coupled-line circuits*. Artech House Publishers.

Muraguchi, M., Yukitake, T., Naito, T. (1983) "Optimum design od 3-dB branch-line couplers using microstrip lines," *IEEE Trans. Microw. Theory Tech.*, vol. 31, no. 8, pp. 674–678.

Pozar, D.M. (1998) *Microwave Engineering*. John Wiley & Sons.

Sans, M., Rodriguez, A., Bonache, J., Boria, V.E., Martin, F. (2014) "Design of planar wideband bandpass filters from specifications using a two-step aggressive space mapping (ASM) optimization algorithm," *IEEE Trans. Microwave Theory Tech.*, vol. 62, no. 12, pp. 3341–3350.

Shahroury, F.R., Wu, C.-Y. (2008) "The design of low LO-power 60-GHz CMOS quadrature-balanced self-switching current-mode mixer,"*IEEE Microw. Wireless Comp. Lett.*, vol. 18, no. 10, pp. 692–694.

Toivanen, J.I., Rahola, J., Makinen, R.A.E., Jarvenpaa, S., Yla-Oijala, P. (2010) *Gradient-based antenna shape optimization using spline curves*. Annual Rev. Prog. Applied Comp. Electromagnetics, Tampere, Finland, pp. 908–913.

Wang, Y., Ke, M., Lancaster, M.J. (2009) "Micromachined millimeter-wave rectangular-coaxial branch-line coupler with enhanced bandwidth," *IEEE Trans. Microw. Theory Tech.*, vol. 57, no. 7, pp. 1655–1660.

Wincza, K., Gruszczynski, S. (2011) "Asymmetric coupled-line directional couplers as impedance transformers in balanced and n-way power amplifiers," *IEEE Trans. Microw. Theory Tech.*, vol. 59, no. 7, pp. 1803–1810.

Wincza, K., Gruszczynski, S. (2016) "Broadband integrated 8×8 Butler matrix utilizing quadrature couplers and Schiffman phase shifters for multibeam antennas with broadside beam," *IEEE Trans. Microw. Theory Tech.*, vol. 64, no. 8, pp. 2596–2604.

Wong, F.-L., Cheng, K.-K.M. (2011) "A novel, planar, and compact crossover design for dual-band applications," *IEEE Trans. Microw. Theory Tech.*, vol. 59, no. 3, pp. 568–573.

Xu, H.-X., Wang, G.-M., Lu, K. (2011) "Microstrip rat-race couplers," *IEEE Trans. Microw. Mag.*, vol. 12, no. 4, pp. 117–129.

Yao, J.J. (2010) "Nonstandard hybrid design with branch-line structures," *IEEE Trans. Microw. Theory Tech.*, vol. 58, no. 12, pp. 3801–3808.